Journal of Molecular Liquids 351 (2022) 118657

Contents lists available at ScienceDirect

Journal of Molecular Liquids

journal homepage: www.elsevier.com/locate/molliq

A computational study of polydimethylsiloxane derivatives as a semi-permeable membrane for in-field identification of naphthenic acids in water using portable mass spectrometry

Stevan Armaković [a,*], Đorđe Vujić [b], Boris Brkić [b,*]

[a] University of Novi Sad, Faculty of Sciences, Department of Physics, Trg D. Obradovića 4, 21000 Novi Sad, Serbia
[b] University of Novi Sad, Biosense Institute, Dr Zorana Đinđića 1, 21000 Novi Sad, Serbia

ARTICLE INFO

Article history:
Received 17 December 2021
Revised 15 January 2022
Accepted 28 January 2022
Available online 01 February 2022

Keywords:
polydimethylsiloxane (PDMS)
Mass spectrometry
Molecular dynamics
Density functional theory
Density functional tight binding
Noncovalent interactions

ABSTRACT

A detailed computational study has been performed to assess the possibility of applying polydimethylsiloxane (PDMS) and its structurally similar derivatives as semi-permeable membranes to filter two naphthenic, cyclohexanecarboxylic and 2-norbornaneacetic, acids using a portable mass spectrometer. Several state-of-the-art levels of theory have been used to understand the interactions between PDMS membranes and naphthenic acids, which enabled us to consider membrane design in both liquid and gas phases. Molecular dynamics (MD) simulations have been performed to evaluate interaction energy between PDMS-based layers and naphthenic acids in the presence of water molecules, a scenario that corresponds to the most realistic conditions. Density functional tight-binding (DFTB) calculations were used to obtain interaction energies between PDMS-based chains and naphthenic acids, which allowed us to consider interaction in the gas phase. Density functional theory (DFT) calculations were used to investigate the electron density between the interacting molecular species, which was the basis to identify noncovalent interactions responsible for the interaction and binding between PDMS-based chains and naphthenic acids. Finally, the symmetry-adapted perturbation theory (SAPT) approach was used to decompose the interaction energies into meaningful physical components and identify the one that principally contributes to the attraction. Our calculations indicate that PDMS and some of its structurally similar derivatives have significant potential to be practically applied as semi-permeable membranes for filtration of cyclohexanecarboxylic and 2-norbornaneacetic acids.

1. Introduction

The high demand for hydrocarbons and excess consumption are depleting conventional oil extraction sites. Oil deposits rich with naphthenic acids are becoming interesting in terms of exploitation as their availability and relatively low price make them a viable raw material [1]. Crude oil rich with naphthenic acids is found primarily at sites in California, Russia, Venezuela, China and India [2]. The acidity of a crude oil presents concern in the oil industry because equipment used in oil extraction and refining is subjected to increased wear. Therefore, the possibility of breakdowns brings up maintenance costs of the facilities which will cause higher market prices as a consuequece [3].

Structurally, naphthenic acids are monocarboxylic acids with carboxyl group attached to a cyclopentane or cyclohexane ring either directly or via alkyl group with the total number of carbon atoms ranging from 7 to 17 and in some cases up to 40 [4,5]. Acidity of a crude oil is expressed using TAN, which is a total acid number. TAN is expressed as quantity of base, potassium hydroxide in milligrams, needed for neutralization of 1 g of crude oil [6]. It is now known that there is a link between TAN and corrosive properties of a crude oil [7], but it cannot be used as definite claim since crude oils have different corrosive characteristics and can have the same TAN value [8]. This leads to a conclusion that not all acids contribute to the corrosion equally. Crude oil has naphthenic acid content in range usually from 0 to 4% [9].

Another other major issue with naphthenic acids-rich oil deposits is that naphthenic acids are relatively soluble in water (50 mg L^{-1}) [10] which creates a range of an ecological problems for the wildlife in case of oil spills. Toxicity of just few dozens of naphethenic acids have been studied since not so many of these compounds are available commercially, and it has been proven for a wide range of organisms such as birds, bacteria, aquatic and terrestrial animals [5,11].

* Corresponding authors.
E-mail addresses: stevan.armakovic@df.uns.ac.rs (S. Armaković), boris.brkic@biosense.rs (B. Brkić).

https://doi.org/10.1016/j.molliq.2022.118657
0167-7322/

Monitoring of crude oil spills on-site became possible by using membrane inlet mass spectrometry (MIMS) [12]. This technique is based on having semi-permeable membranes between an analyzed medium and a vacuum system with the analyzer. MIMS is simple, requires no sample preparation and is highly sensitive for certain types of volatile organic compounds from aqueous, gaseous and solid samples [13].

MIMS coupled with a portable mass spectrometer could potentially be cost-effective, simple and easy method [14] of analyzing naphthenic acids in oil spills. Most of the tested naphthenic acids have mass range up to m/z 200, and they could be detected with a suitable MIMS membrane.

The development of novel materials for application in various areas heavily relies on computational methods. To understand what happens on the molecular level, scientists apply a variety of atomistic computations that enable them to predict the essential properties and reduce the cost related to experiments [15–18].

To pass through the MIMS membrane, the interaction energy between membrane and molecule needs to be as low as possible. If the interaction energy between SPM and molecule is too strong, the SPM could practically trap the molecule, preventing it from reaching the detector. In this regard, it is imperative to identify materials with as weak as possible interaction energy with the molecule that should be detected. This is where computational methods such as molecular dynamics (MD) simulations and quantum mechanical (QM) calculations are beneficial because they enable evaluating the interaction energy between membrane and molecule.

Polymer-based membrane materials are used for MIMS due to their selectivity for a broad range of volatile and semi-volatile organic compounds. They provide fast chemical analysis (within seconds) allowing both qualitative and quantitative analysis with limited or no sample preparation. This is enabled with a pervaporation process for the analytes consisting of adsorption of molecules onto a membrane surface, diffusion through the membrane material and desorption of the analyte into the mass spectrometer.

Thanks to the rapid development of science and technology, various computational methods have become readily available for the investigation of materials' properties long before they are synthesized [19–24]. Quantum-mechanical methods, fundamentally based on the density functional theory (DFT), are among the most frequently utilized levels of theory. They have been beneficial for predicting the strength of binding between molecules [25–28]. Computational methods based on wavefunction offer even more accurate results, at the cost of computational time necessary to perform these calculations [20,29]. Although solvent effects can be treated by DFT and wavefunction methods with a variety of approaches, to involve solvent molecules explicitly, it is more feasible to use molecular dynamics (MD) simulations [17,21,29,30]. Aside of allowing explicit involvement of solvent molecules, it also enables one to study large systems consisting of thousands of atoms.

This work aims to apply state-of-the-art computations to evaluate the potential of PDMS and structurally similar polymers to be used as semi-permeable membranes for cyclohexanecarboxylic (CHA) and 2-norbornaneacetic (2NA) naphthenic acids. This work encompasses the application of MD simulations, density functional theory (DFT), density functional tight-binding (DFTB) and symmetry-adapted perturbation theory (SAPT) calculations. MD simulations were used to consider the interaction between PDMS and naphthenic acids in the most realistic conditions, where the polymer layer and interacting molecule are surrounded by water. DFTB calculations were used to obtain interaction energies between PDMS-based polymeric chains and naphthenic acids, which correspond to conditions in the gas phase. Finally, to gain a deeper understanding of the interaction between PDMS and naphthenic acids, a set of DFT and SAPT calculations has been performed. All calculations are investigating the potential of the pure PDMS as a semi-permeable membrane and indicate that one of its derivatives may have better membrane properties for fast separation of naphtenic acids.

2. Computational details

In this work, several modern molecular modeling packages have been utilized to study the interactions between PDMS-based materials and selected naphthenic acids. MD simulations were performed with the Desmond [31] program, as implemented in the Schrödinger Materials Science Suite (SMSS), version 2019-3 [32–35]. The OPLS3e force field [36–39] was used in all MD simulations, while the simulation time was set to 30 ns. Other MD simulation details included the application of the NPT ensemble of particles and normal pressure, while the solvent was modeled by a simple point charge (SPC) model. The models used for MD simulations are illustrated in Fig. 1. MD models consisted of the membrane part, on which top was placed one molecule of naphthenic acid (CHA or 2NA). The membrane part and the naphthenic acid molecules were then surrounded by water molecules to mimic the realistic situation corresponding to the spiling of oil into the water. The packing of the polymer chains, which constitute the central part of the MD model, was performed with the Packmol program [40,41]. 10 MD models were subjected to MD simulations at three temperatures. Further details about MD models and selected temperatures are provided in the chapter dealing with MD results.

Quantum mechanical (QM) calculations have been performed using the density functional theory (DFT), density functional tight-binding (DFTB), and symmetry adapted perturbation theory (SAPT) methods. DFT calculations in combination with B3LYP exchange-correlation functional [42], a standard functional for initial studying of reactive and interaction properties of small and middle-sized organic molecules, and 6-31G(d,p) basis set [43–45] were used to investigate the reactive properties of CHA and 2NA molecules. To investigate the interaction between PDMS and its derivatives with CHA and 2NA molecules, a combination of DFTB and DFT calculations has been used. DFTB [46–48] calculations based on the extended tight-binding (xTB) model Hamiltonian and GFN1-xTB parametrization covering elements up to radon were used to optimize systems consisting of polymer chain plus CHA or 2NA molecules. This variant of DFTB, recently developed by Grimme et al. [49], allows one to perform various QM calculations at a fraction of time compared to the DFT approach. Interaction energies between polymer chain and naphthenic acid molecules were calculated based on DFTB calculations according to the following equation:

$$E_i = E_{tot}(PDMS + NA) - E(PDMS) - E(NA), \quad (1)$$

where $E_{tot}(PDMS + NA)$ denotes total energy of optimized complex consisting of PDMS-based chain plus the CHA or 2NA molecule, $E(PDMS)$ denotes total energy of sole optimized PDMS-based chain, while the $E(NA)$ denotes the total energy of CHA or 2NA molecule.

Furthermore, the geometrically optimized structures were exported and used to identify noncovalent interactions between PDMS and naphthenic acids molecules by DFT calculations. Last but not least, SAPT [50–53] calculations (precisely the SAPT0 variant) were used on selected systems to decompose the interaction energy to meaningful physical components, revealing which contribution was the most important in terms of attraction between polymer chains and CHA/2NA molecules. In the framework of the SAPT approach, the dimer's Hamiltonian is fragmented to contribu-

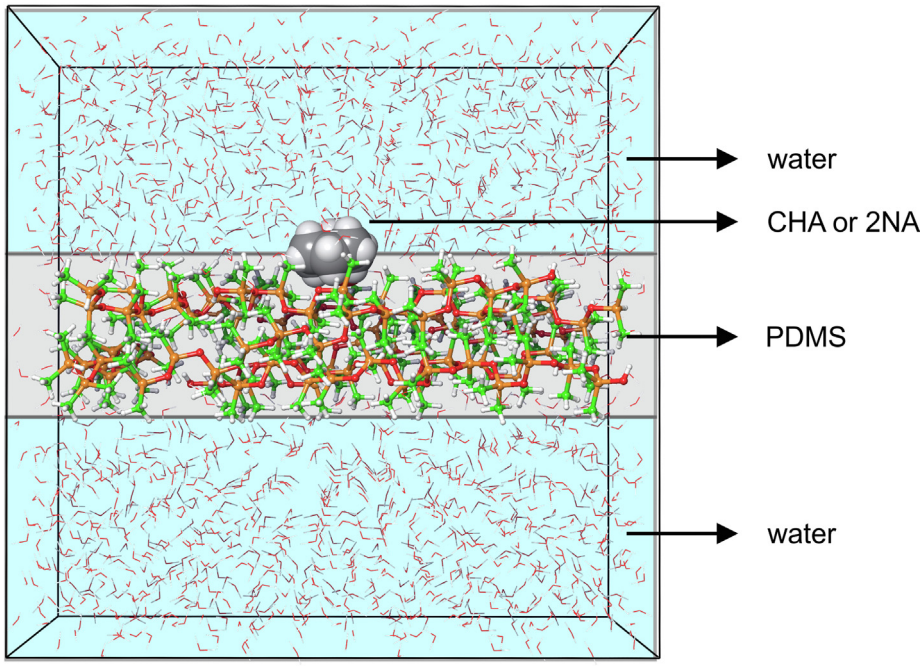

Fig. 1. Model for MD simulations – PDMS chains are presented in ball-and-stick representation, CHA or 2NA as van der Waals spheres, while water molecules are shown in the wired presentation.

tions from each monomer and the interaction. In particular, the Hamiltonian is written as a sum of the monomer Fock operators, monomers' fluctuation potentials, and the interaction potential. The SAPT0 variant represents the simplest truncation of the SAPT expansion.

All DFT calculations have been performed with the Jaguar [32,33] programs, as implemented in the SMSS, version 2021-4. All DFTB calculations have been performed with the DFTB engine, as implemented in the Amsterdam Modeling Suite 2021.1 developed by Software for Chemistry and Materials (SCM) [54]. SAPT0 calculations were performed with the PSI4 program [55,56].

In all cases, the default convergence criteria have been used for self-consistent field procedure and geometrical optimizations have been used. Maestro GUI was used to prepare input files and visualize results in cases of DFT calculations and MD simulations, while the AMS GUI was used to prepare input files and visualize results in the case of DFTB calculations. Input files for the PSI4 modeling package were made with the help of the Avogadro program [57,58].

3. Results and discussion

3.1. Models for MD simulations and QM calculations

In this study, the MD simulations had priority since they allow modeling of the interaction between membrane material and selected molecules in the presence of water. The presence of water corresponds to a realistic situation such as on-site monitoring of NA concentration. This is due to environmental accidents such as oil spilling in the ocean or other water. The MD model used throughout this study is illustrated in Fig. 1.

In Fig. 1, the central part (grey region) contains the layer of PDMS chains. In this case, the PDMS layer had 8 PDMS chains, each consisting of 12 monomers of PDMS. On top of the PDMS layer, the CHA or 2NA molecules were placed. PDMS layer with CHA or 2NA molecules is surrounded by layers of water (light blue region). In all cases, the MD model was of cubic shape, with a side length ranging between 40 Å and 43 Å.

Besides pure PDMS, four other polymers were considered as membranes and filters for CHA and 2NA molecules. In other words, five different polymers were placed in the central region of the model presented in Fig. 1. This means that a total of 10 MD systems were generated (five systems against CHA and five systems against 2NA molecules) and subjected to MD simulations. Due to the size, structural formulas of polymer chains used for MD simulations have been presented in Figure S1 of the Supplementary Materials. To consider the influence of temperature, each of the 10 MD systems was considered at three different temperatures, leading to the fact that 30 MD simulations were performed.

The MD simulations provided a very important parameter – interaction energy between polymer layer and CHA (or 2NA) molecules. However, these values have no practical significance since there are no reference values, which would help us to determine whether the interactions between considered polymers and naphthenic acids are too strong or not.

To find the reference values and validate the model presented in Fig. 1, it was necessary to place benzene and isophorone molecules on top of the polymer layer, calculate the interaction energies, and use them as reference values. Literature survey has revealed experiments in which it was demonstrated that benzene [59] and isophorone [14] could easily pass through the PDMS membrane. Therefore, if the binding energy between the PDMS and benzene (or binding energy between PDMS and isophorone) is similar to binding energy between PDMS and CHA (or 2NA), it means that PDMS can be potentially employed as a material for the development of membranes/filters for CHA and 2NA.

To be applied as a membrane through which molecule can pass, the interaction energy between the polymer layer and molecule needs to be as low as possible because too high interaction energies would practically trap the molecule and prevent it from reach-

Table 1
Polymer names and their abbreviations considered in this work.

Polymer	Abbreviation used
Poly(dimethylsiloxane	PDMS
Poly(dimethylsiloxane), hydride terminated	PDMS-HDT
Poly(dimethylsiloxane), bis(3-aminopropyl) terminated	PDMS-B3T
Poly(dimethylsiloxane), monohydroxy terminated	PDMS-MHT
Poly(dimethylsiloxane-co-methylhydrosiloxane), trimethylsilyl terminated	PDMS-TMT

ing the detector. This means that we searched for polymer layer with as low as possible interaction energy against CHA/2NA.

The names and corresponding abbreviations of polymers selected as membrane constituents (central part in Fig. 1) are summarized in Table 1, while Fig. 2 contains their 3D structures.

Polymer chains used for QM calculations are presented in Fig. 2, and they are slightly shorter than the chains used for MD simulations to reduce the computational cost. In particular, QM polymer chain models consisted of 6 monomer units, while in the case of the MD simulations, they consisted of 8 monomer units. In the case

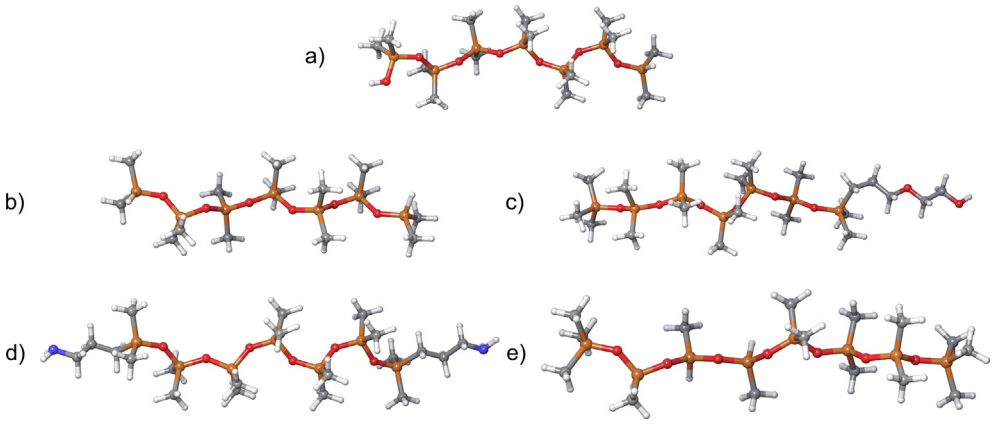

Fig. 2. Structures of polymer chain models used for QM calculations a) PDMS, b) PDMS-HDT, c) PDMS-B3T, d) PDMS-MHT and e) PDMS-TMT.

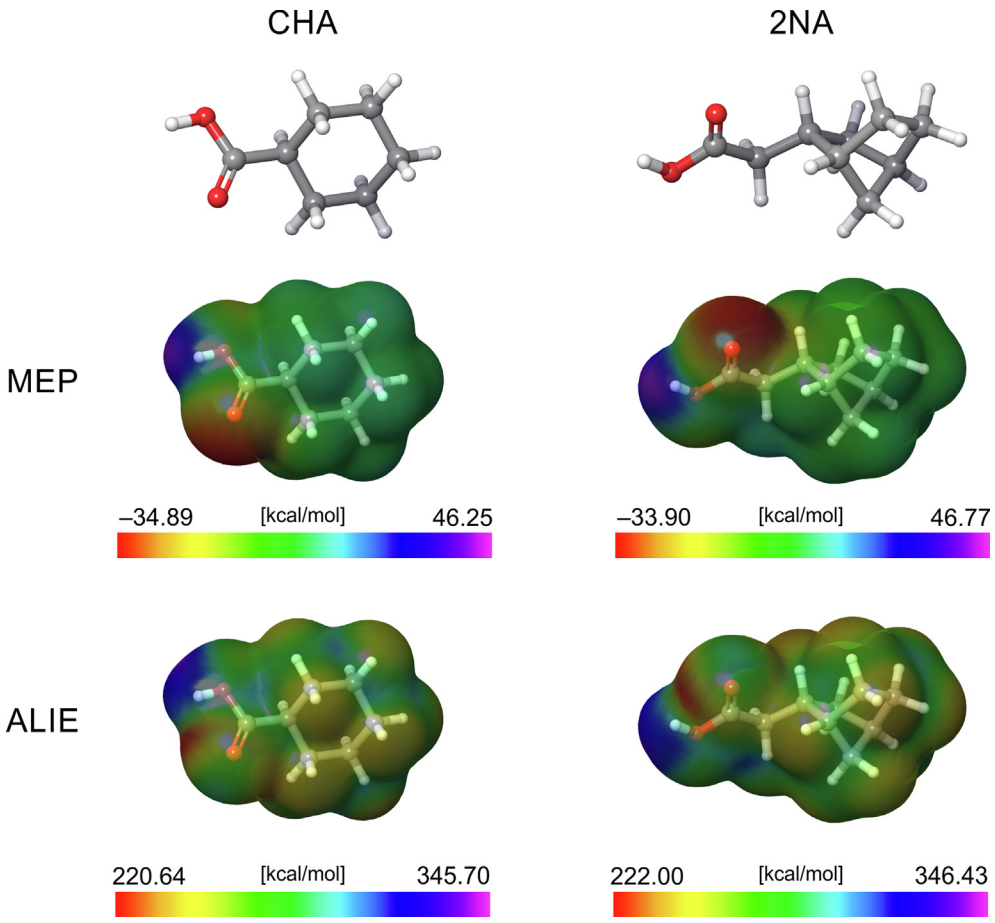

Fig. 3. Geometrically optimized structures of CHA and 2NA and the corresponding MEP and ALIE surfaces.

of QM calculations, above each polymer chain, CHA or 2NA molecule was placed, and then the geometrical optimizations were performed at DFTB/GFN1-xTB level of theory.

3.2. Selection of naphthenic acids and their reactivity

In this work, the PDMS-based polymers were considered to be applied for CHA and 2NA naphthenic acids. The reason for selecting these naphthenic acids was that the cyclic naphthenic acid are less prone to biodegradation than acyclic fatty acids [60], therefore it is more likely to find them *in situ*. Fig. 3 contains the geometrically optimized structures of CHA and 2NA molecules, together with their molecular electrostatic potential (MEP) and average local ionization energy (ALIE) surfaces.

MEP and ALIE have been established as standard quantum-molecular descriptors explaining the local reactivity of molecules [61–65]. MEP descriptor is frequently used to identify molecular sites prone to interact with other molecules based on electrostatic interactions. On the other side, ALIE is intended to identify molecular areas prone to losing an electron if adequate energy is provided, revealing the molecular sites susceptible to electrophilic attacks. If the values of MEP and ALIE for CHA and 2NA are considered, it can be stated that these two molecules have very similar reactivity. The values and distribution of MEP and ALIE are almost the same in both cases. The magnitude of negative MEP value of CHA (-34.89 kcal/mol) is somewhat higher than the 2NA (−33.90 kcal/mol), while the difference in the case of positive MEP values is even lower. Concerning the distribution, in both cases, the near vicinity of the oxygen atom is characterized by the lowest MEP values. In contrast, the hydrogen atom of the OH group is characterized by the highest MEP values, identifying these two molecular sites as the most reactive with other molecules based on electrostatic interactions.

The same qualitative and quantitative picture is revealed in the case of the ALIE descriptor. Again, both molecules have very similar minimal and maximal ALIE values. In contrast, the minimum value is located within the carboxyl group, between its oxygen atom and the hydrogen atom of the OH group. The acquired information about the reactivity of CHA and 2NA is essential for the understanding of the interaction with the PDMS and its derivatives and will be used later in the manuscript. Both MEP and ALIE surfaces have been obtained with *iso*-value set to 0.001.

3.3. Interaction energies based on MD simulations

We rely on the interaction energy calculation to identify whether the PDMS could be applied to develop membranes for CHA and 2NA molecules. To be suitable for these purposes, the interaction energies between PDMS and CHA/2NA should be as low as possible because that would allow CHA and 2NA to pass through the membrane.

Therefore, to obtain the reference values of the interaction energies, the MD simulations were first performed when the BEN, ISO, CHA and 2NA were placed on top of the polymer layer, which consisted of pure PDMS. These results are summarized in Table 2.

The results of the first four MD simulations presented in Table 3 were very encouraging for the potential application of PDMS as membrane material in the case of the CHA and 2NA molecules. Namely, the lowest interaction energy has been calculated in the case of the BEN molecule (−5.867 kcal/mol), meaning that this molecule could easily pass through the PDMS membrane. This experimentally confirmed fact was somewhat expected due to the very small size of the BEN molecule and known reactivity. The interaction energy between PDMS and ISO was calculated to be −9.120 kcal/mol, significantly higher than the BEN. However, it has been experimentally established that PDMS membranes are applicable in the case of the ISO molecule, so the value of −9.120 kcal/mol can be regarded as the reference value. In other words, for some molecule to be able to penetrate through the PDMS membrane, its interaction energy should not exceed −9.120 kcal/mol (i.e. taking into account the MD simulation parameters used in this study). Of course, this does not preclude higher magnitudes of interaction energy; however, they should not be too much higher.

Results in Table 3 show that the interaction energy between PDMS and CHA is much lower than the reference value of −9.120 kcal/mol, indicating that the CHA molecule could penetrate the PDMS membrane. The obtained result regarding 2NA is also encouraging because the magnitude of interaction energy with PDMS at 300 K is higher for just 0.5 kcal/mol. There is also a relatively significant difference in the interaction energies of CHA and 2NA with PDMS, although there is no significant difference in the local reactivity of theses molecules. The initial explanation for this observation can be found by analyzing the structures of these molecules. Namely, the 2NA has one rotatable bond more than CHA, meaning that it is a slightly more flexible molecule. This flexibility might lead to a higher possibility to involve reactive centers (the oxygen atom and hydrogen atom of the OH group) in noncovalent interactions with PDMS.

After establishing that a pure PDMS according to our MD simulations might be applicable in the case of CHA and 2NA molecules, the next step was to check the interaction energies for some other polymers and identify the ones with the lowest interaction energies against CHA and 2NA. The criteria for selecting polymers were that they are relatively simple modifications of the pristine PDMS, aiming to understand how subtle changes in polymer structure affect their ability to filter the selected molecules. The interaction energies between PDMS-related polymers and CHA/2NA molecules are summarized in Fig. 4, including the temperature dependence.

The specific different temperatures in Fig. 4 were selected to cover realistic environmental conditions during the oil spill in oceans and for the design of detectors of CHA and 2NA. The first

Table 2
Interaction energies [kcal/mol] between PDMS and BEN, ISO, CHA and 2NA, according to MD simulations at 300 K.

	BEN	ISO	CHA	2NA
PDMS	−5.867	−9.120	−8.107	−9.641

Table 3
DFTB interaction energies between PDMS and BEN, ISO, CHA and 2NA (grey background denotes conformations near terminating fragments).

Polymer chain	Interaction energies for different configurations					Mean binding energies	
	#1	#2	#3	#4	#5	$\bar{E}_i^{s+t}$	$\bar{E}_i^{s}$
PDMS + BEN	−1.95	−4.54	−3.56	−2.21	−0.28	−2.51	−3.35
PDMS + ISO	−6.96	−7.12	−2.82	−2.42	−5.55	−4.97	−5.63
PDMS + CHA	−9.72	−1.14	−10.00	−10.15	−7.05	−7.61	−6.95
PDMS + 2NA	−3.51	−0.95	−10.57	−9.41	−8.89	−6.67	−5.01

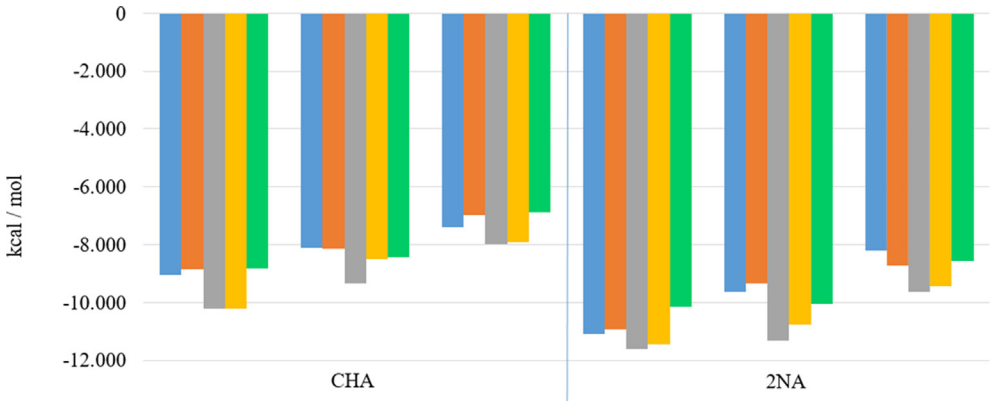

	276 [K]	300 [K]	343 [K]	276 [K]	300 [K]	343 [K]
PDMS	-9.048	-8.107	-7.396	-11.073	-9.641	-8.194
PDMS-HDT	-8.845	-8.130	-6.972	-10.926	-9.336	-8.717
PDMS-B3T	-10.216	-9.343	-7.965	-11.597	-11.316	-9.630
PDMS-MHT	-10.206	-8.500	-7.911	-11.451	-10.759	-9.433
PDMS-TMT	-8.827	-8.428	-6.881	-10.143	-10.053	-8.552

Fig. 4. Overview of interaction energies between PDMS and CHA (2NA) at different temperatures.

two temperatures have been chosen to cover the interval of water temperature within oceans. It has been established that ocean temperature ranges from 271 K to 303 K, which is heavily dependent on the depth. Although surface water can reach temperatures of 303 K due to the influence of the Sun, the average temperature of an ocean is around 276 K, because the Sun's rays cannot penetrate deeper than 1000 m. This explains why we have chosen to perform our MD simulations at 276 K and 300 K.

The highest temperature in Fig. 4, was selected since it is known that the sensitivity of PDMS increases with the temperature [66], and it gives a stable sensor signal up to temperatures of 343 K [67]. Therefore, if it is a goal to develop a detector for CHA or 2NA with higher working temperature, this temperature is also of interest. Concerning the CHA and 2NA, the temperature of 343 K is acceptable because their boling points are $\sim$ 504 K and $\sim$ 683 K, respectively [68,69].

We will first elaborate the MD results at 300 K. In the case of the CHA molecule, MD results gave interaction energies whose magnitudes are lower than the reference value obtained in Table 3. Only in the case of the PDMS-B3T polymer, the magnitude of interaction energy was just slightly higher (for just 0.2 kcal/mol) than the reference value, meaning that this derivative also has potential for practical applications. The situation is noticeably different for 2NA molecule, where the magnitude of the interaction energy is considerably higher than the reference value of −9.120 kcal/mol in all cases but PDMS-HDT. In this case, the interaction energy is just slightly higher ($\sim$0.2 kcal/mol), and it certainly has the potential to be considered a suitable polymer material for 2NA.

Considering the influence of temperature results in Fig. 4, the magnitude of the interaction energy between PDMS polymers and CHA/2NA molecules decreases with temperature increase in all cases. In other words, to ensure that CHA or 2NA could penetrate easier the PDMS-related membranes, it is desirable to increase the system's temperature. This is consistent with the experimental fact that the sensitivity of PDMS increases with the increase of temperature.

Next, it should be noticed that the interaction energies of PDMS-HDT and PDMS-TMT with CHA at 276 K are lower than the interaction energy of PDMS with CHA at 300 K. I.e., these two polymers could be a better solution at lower temperatures in case of CHA than the pure PDMS.

MD simulations at 343 K in the case of CHA molecule produced energies significantly lower than the reference value of −9.120 kcal/mol, indicating that practically all considered polymers might be applicable as membranes. The best result is obtained for the PDMS-TMT polymer, in which case the interaction energy against CHA molecule was calculated to be −6.881 kcal/mol. Not only is this value much lower than the reference value obtained for the ISO molecule, but it is also very close to the value of interaction energy between PDMS and BEN molecule.

The increase of temperature to 343 K improved the interaction energies in the case of the 2NA molecule as well. However, the improvement was not as good as in the case of CHA molecule. For three polymers, PDMS, PDMS-HDT and PDMS-TMT, interaction energies with 2NA were lower than the reference value of −9.120 kcal/mol. The remaining two polymers (PDMS-B3T and PDMS) also have potential because they are characterized by slightly higher interaction energies than the reference value.

3.4. Interaction energies based on QM calculations

Apart from MD calculations, the interaction between considered polymers and CHA/2NA molecules was also investigated using the QM calculations. The applied QM calculations were based on DFTB, and DFT approaches without consideration of solvent effects. Due to the computational costs related to QM methods, it is usually feasible to consider the interaction between only one polymer chain (or its fragment) and a selected molecule. Without consideration of solvent effects, these calculations correspond to the gaseous state, which is also essential for developing sensors. Namely, the water samples containing CHA or 2NA could be evaporated and then delivered to a detector system comprising a polymer membrane, among other elements.

Due to the size of the QM systems in this study, $\sim$100 atoms, the QM method of choice was the DFTB combined with GFN1-xTB parametrization. In the DFTB engine of AMS, the mentioned parametrization also includes the D3-BJ dispersion correction by default, making it particularly useful for investigating the noncovalent interactions between molecules.

Next, we present the results of the interaction energies. Again, the first step was to validate the used models and find the reference values that would help us to evaluate whether the considered

polymers might be applicable as membrane materials for CHA and 2NA, this time in the gas state. Therefore, the first task regarding QM calculations was to calculate interaction energies between PDMS and BEN, ISO, CHA and 2NA, and compare them. These results are summarized in Table 5.

Due to different possible orientations of the molecules above the polymer chain, we have performed several geometry optimizations for each system. For those reasons, in Table 5 and the following tables, we report interaction energies for different conformations (#1, #2,...). Conformations #4 and #5 (with the grey background) in Table 5 correspond to systems where molecules have been placed near terminating fragments in starting configurations.

Because of the flexible nature of polymers and different possible orientations of molecules adsorbed on top of them, we are also reporting two types of average interaction energies – average interaction energy including orientations on both side chains and terminating fragments E_i^{s+t}, and average interaction energy including only orientations above the side chains, E_i^s. The reason for this is the fact that the reactivity of side chains and terminating fragments differ. However, if the length of polymers is very long, then the contribution of terminating fragments to the interaction between polymer chains and selected molecules can be neglected. I.e., in such cases, the number of interactions involving terminating fragments is negligible compared to the number of interactions involving side chains. Thus, the results in Table 4, and the following tables, provide information about interactions between polymer chains with CHA or 2NA for two border cases – short and long polymer chains.

Results in Table 5 indicate again that the lowest interaction energy is between PDMS and benzene molecule, taking into account both E_i^{s+t} and E_i^s. ISO molecule again has stronger interaction energy compared to benzene. Thus the values of −4.97 kcal/mol and −5.63 kcal/mol could be considered as border/reference values of interaction energy.

Considering the E_i^{s+t} parameter, both CHA and 2NA have much stronger interaction energies with PDMS compared to ISO molecule. This result indicates that the shorter polymer PDMS chains might not be adequate materials for membranes in the case of CHA and 2NA when considering the gas state. On the other side, the E_i^s for interaction between PDMS and 2NA molecule is much lower than the E_i^s for interaction between PDMS and ISO, indicating that for longer polymer chains, PDMS might be suitable as membrane material for 2NA molecule.

Further, in Tables 6 and 7, we present the results of DFTB interaction energies between other considered polymer chains with CHA and 2NA molecules, respectively. Conformations where CHA and 2NA have been placed near terminating fragments, are again grey-shaded.

Considering the interactions between PDMS-based polymers and CHA molecule, and the $\bar{E}_i^{s+t}$, it seems that the best choice would be the PDMS-TMT derivative. Namely, in this case, the interaction energy is the closest to the border value calculated in the case of the interaction of PDMS with ISO. All other interaction energies in the case of the CHA molecule, considering both $\bar{E}_i^{s+t}$ and $\bar{E}_i^{s}$, are much higher.

Table 4
DFTB interaction energies in [kcal/mol] between PDMS based polymer chains and CHA (grey background denotes conformations near terminating fragments).

Polymer chain	Interaction energies for different configurations						Mean binding energies	
	#1	#2	#3	#4	#5	#6	$\bar{E}_i^{s+t}$	$\bar{E}_i^{s}$
PDMS	−9.72	−1.14	−10.00	−10.15	−7.05	/	−7.61	−6.95
PDMS-HDT	−6.59	−7.53	−13.40	−13.58	−13.58	/	−10.94	−9.17
PDMS-B3T	−11.14	−4.25	−10.59	−15.24	−15.24	/	−11.29	−8.66
PDMS-MHT	−11.11	−5.93	−9.91	−5.99	−13.60	−9.14	−9.28	−8.98
PDMS-TMT	−5.50	−5.82	−13.08	−3.53	−3.53	/	−6.29	−8.13

Table 5
DFTB interaction energies in [kcal/mol] between PDMS based polymer chains and 2NA (grey background denotes conformations near terminating fragments).

Polymer chain	Binding energies for different configurations						Mean binding energies	
	#1	#2	#3	#4	#5	#6	$\bar{E}_i^{s+t}$	$\bar{E}_i^{s}$
PDMS	−3.51	−0.95	−10.57	−9.41	−8.89	/	−6.67	−5.01
PDMS-HDT	−5.77	−6.35	−13.69	−2.96	−2.96	/	−6.35	−8.60
PDMS-B3T	−3.99	−2.79	−8.89	−18.44	−18.44	/	−10.51	−5.23
PDMS-MHT	−10.60	−3.39	−12.24	−6.65	−10.22	−8.39	−8.58	−8.74
PDMS-TMT	−5.72	−12.15	−13.89	−4.29	−4.29	/	−8.07	−10.59

Table 6
Strength of noncovalent interactions expressed in terms of electron density [e/bohr^3].

	H1	*H2*	*O1*	*Total # NCI*
PDMS & CHA	−0.0138	−0.0176	−0.0251	6
PDMS & 2NA	−0.0115	−0.0148	−0.0236	11
PDMS-HDT & CHA	−0.0148	−0.0181	−0.0286	10
PDMS-HDT & 2NA	/	−0.0237	−0.0264	8
PDMS-TMT & CHA	−0.0079	−0.0150	−0.0248	13
PDMS-TMT & 2NA	−0.0074	−0.0144	−0.0250	16

The situation is much better in the case of the interaction between PDMS-based polymers and 2NA molecule. $\bar{E}_i^s$ values in case of the interaction between PDMS and 2NA, and PDMS-B3T and 2NA, are lower than the $\bar{E}_i^s$ values in case of the interaction between PDMS and ISO. This means that for longer polymer chains, both pure PDMS and PDMS-B3T might be good choices when developing membranes for 2NA.

3.5. Identification of noncovalent interactions

To better understand the attractive interaction between PDMS-based polymers from one side and CHA and 2NA molecules from the other side, we have performed DFT calculations to identify and quantify noncovalent interactions that are principally contributing. The identification of the noncovalent interactions in this work is based on the electron density analysis according to the ref-

Table 7
SAPT0 components and charge transfer.

Systems	*EL*	*EX*	*I*	*D*	T_{SAPT0}
PDMS & CHA	−26.06	37.40	−9.21	−12.08	−9.94
PDMS & 2NA	−24.23	38.12	−9.18	−14.52	−9.82
PDMS-HDT & CHA	−32.83	45.08	−11.91	−14.13	−13.80
PDMS-HDT & 2NA	−28.76	42.22	−10.99	−14.10	−11.63
PDMS-TMT & CHA	−22.89	36.61	−7.61	−14.85	−8.74
PDMS-TMT & 2NA	−22.79	36.77	−8.47	−16.45	−10.94

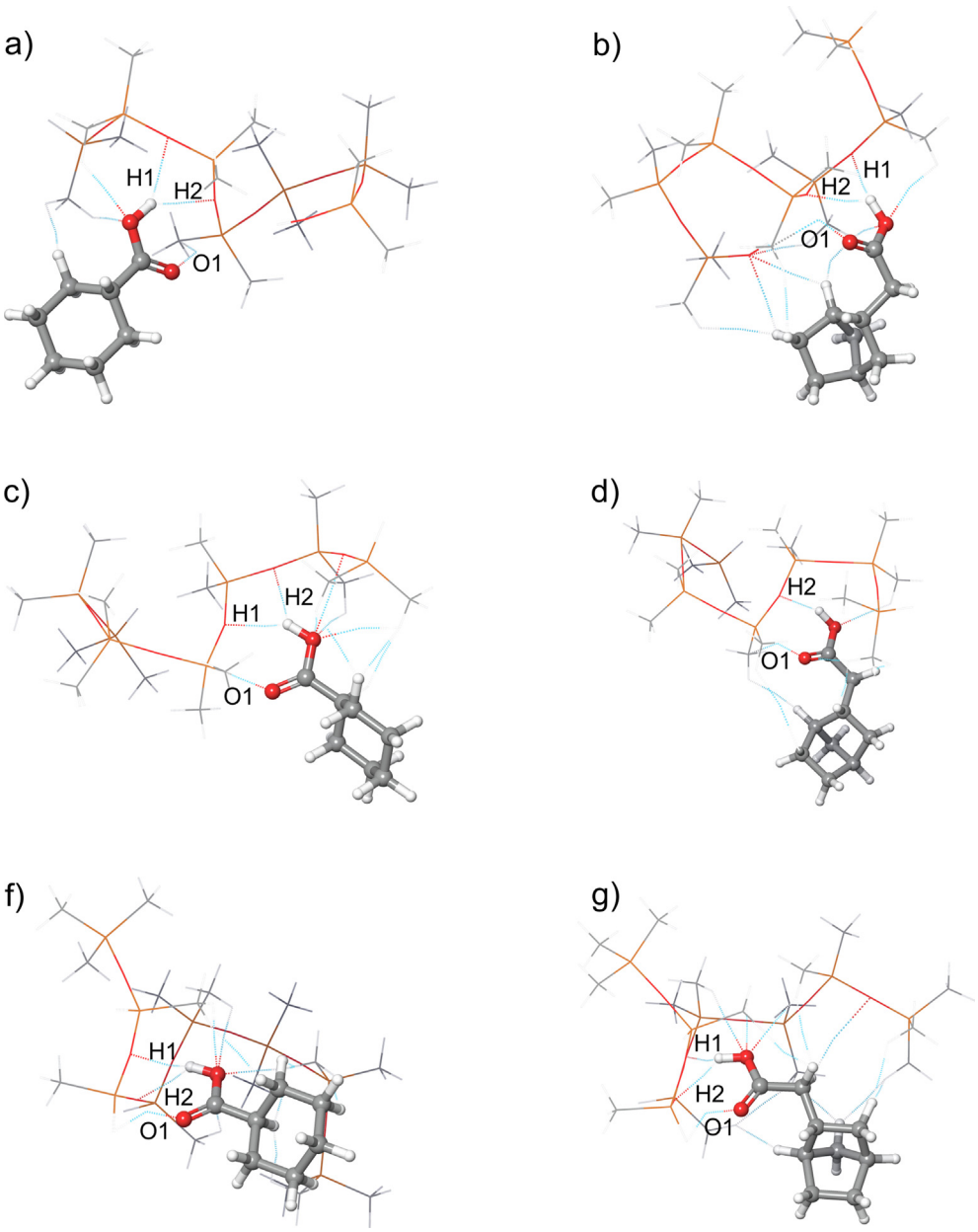

Fig. 5. Noncovalent interactions between PDMS-based polymer chains and CHA/2NA molecules for conformation 3: a) PDMS & CHA, b) PDMS & 2NA, c) PDMS-HDT & CHA, d) PDMS-HDT & 2NA, e) PDMS-TMT & CHA, f) PDMS-TMT & 2NA.

erences [70,71], and the method explained therein is incorporated in the Jaguar program of the SMSS modeling package. Previously, DFTB optimized structures have been exported from AMS and imported to SMSS.

In Fig. 5 all intermolecular noncovalent interactions between PDMS-based polymer chains and CHA/2NA molecules have been illustrated. Analysis of the interaction energies suggests that conformations #3 are characterized with the strongest interaction energies, therefore these conformations have been selected for the analysis of noncovalent interactions. Taking into account both MD and QM results, PDMS, PDMS-HDT and PDMS-TMT have the highest potential for practical applications, so these systems interacting with naphthenic acids were selected for analysis of the noncovalent interactions. The strongest noncovalent interactions are denoted in Fig. 5, and their strengths have been summarized in Table 6.

For the sake of clarity, Fig. 5 contains only intermolecular noncovalent interactions. Polymer chains have been displayed in wire representation, while CHA and 2NA molecules have been displayed in ball-and-stick representation. Noncovalent interactions involving hydrogen atoms of the OH group of CHA and 2NA have been named H1 and H2, while the noncovalent interactions involving the oxygen atom of the carboxyl group have been named O1.

Local reactivity properties analyzed through MEP and ALIE descriptors indicated the importance of the carboxyl group in terms of interactions with other molecules. The analysis of noncovalent interactions confirms this as well, since all specific and the strongest noncovalent interactions involve atoms of this group. However, the results regarding noncovalent interactions reveal one more exciting property in the case of QM calculations. Namely, the PDMS-TMT derivative has the weakest specific noncovalent interactions, but the interaction energies are still strong. By counting the number of NCIs for conformation #3, it was concluded that the highest number of NCIs formed precisely when CHA and 2NA interacted with PDMS-TMT (13 and 16, respectively). Since the specific noncovalent interactions are the weakest, in this case, the conclusion is that the high number of noncovalent interactions involving hydrogen atoms of cyclohexane and norbornane fragments are responsible for the strong interaction. The norbornane fragment of 2NA has a much higher number of hydrogen atoms than CHA, leading to the highest number of noncovalent interactions when 2NA interacted with PDMS-TMT.

3.6. Decomposition of the interaction energy

The geometries analyzed in the previous sub-chapter have also been subjected to SAPT0 calculations. This method is useful for calculating the noncovalent interaction in the so-called direct way, i.e. interaction energy is calculated without calculations of total energies of complex and constituents of that complex. Also, this method is used for the decomposition of interaction energy into physical components. These components are electrostatic (EL), exchange (EX), induction (I) and dispersion (D) components. All components but EX are attractive. Therefore, by SAPT calculations and careful comparison of interaction energy components, one can identify the most critical aspects of attractive interactions between molecules. SAPT0 components together with total SAPT0 interaction energies (T_{SAPT0}) are summarized in Table 7.

Considering results from both MD simulations and QM calculations, PDMS-TMT derivative seems to have significant potential for further consideration as a possible polymer membrane material in cases of CHA and 2NA. Therefore, we focus special attention on what happens with the SAPT0 components in case of the interaction of this polymer chain with CHA and 2NA. Results in Table 7 indicate that of the attractive components, the magnitudes of *EL* and *I* components are the lowest of all considered, while the magnitude of the *D* component is the highest.

The structure of PDMS-TMT is modified so that half of the chain contains hydrogen atoms instead of methyl groups. Therefore, the substitution of the methyl groups with hydrogen atom connected to silicon atom decreases the potential of the PDMS polymer chain to interact based on electrostatic interactions and increases its potential to interact based on the quantum mechanical force. It is important to remember D component represents quantum mechanical force related to the correlation between electrons of interacting molecules. As if the substitution of the methyl group with hydrogen atom increases the electron density between PDMS chain and naphthenic acid molecule, so the electron correlation is more significant. To test this, we refer to the electronegativities and calculated atomic electrostatic potential charges (Fig. 6).

Electronegativity is a tendency of an atom to attract a bonding electron pair. The higher this value is, the more it will attract a bonding electron pair. In the case of the methyl group, C atoms have higher electronegativity (2.55) than hydrogen (2.20). Therefore, a higher electron density is associated with a carbon atom,

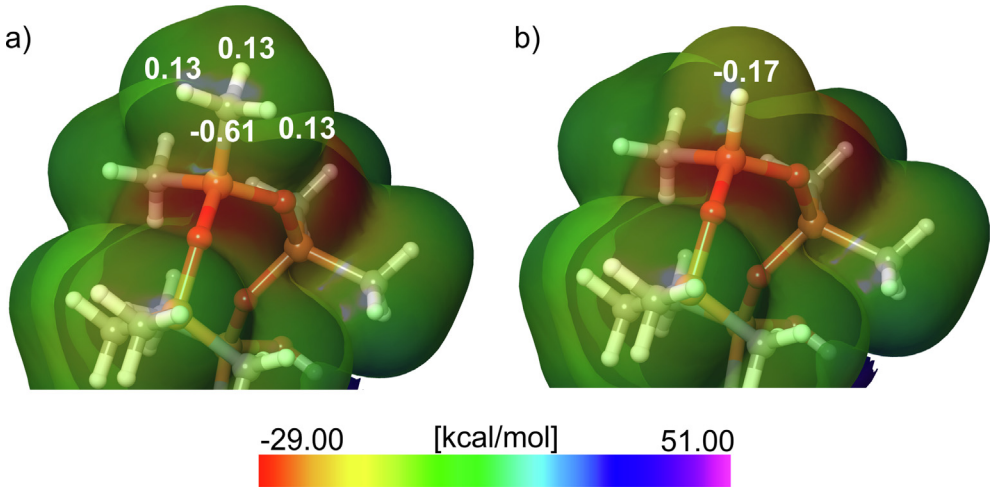

Fig. 6. MEP surface and EPS atomic charges [e] of a fragment of a) PDMS and b) PDMS-TMT chains.

leaving electron deficient hydrogen atoms to interact with naphthenic acid molecules. The situation is quite different in the case of the PDMS-TMT when instead of a methyl group, a hydrogen atom is attached directly to the silicon atom. The electronegativity of hydrogen (2.20) is higher than the electronegativity of silicon (1.90), because of which higher electron density is located near hydrogen atom, which interacts with naphthenic acid molecules. This explains why there is a higher electron correlation when PDMS-TMT interacts with naphthenic acid molecules. These facts are also confirmed by the analysis of MEP surface and ESP atomic charges.

In Fig. 6a it can be seen that hydrogen atoms of the methyl group, which interact with the naphthenic acid molecules, have positive atomic charges. On the opposite, the hydrogen atom directly attached to the silicon atom (PDMS-TMT in Fig. 6b) is characterized by the negative atomic charge (-0.17 e). MEP surface in the case of the PDMS is green in the vicinity of methyl group hydrogen atoms, while it is yellow in the case of the hydrogen atom of the PDMS-TMT, indicating negative values of electrostatic potential. This also confirms that in the case of the PDMS-TMT, higher electron density interacts with the naphthenic acid molecules, thus explaining higher electron correlation and higher magnitude of the D component.

4. Conclusions

This paper evaluated the potential for practical applications of selected PDMS derivatives in portable mass spectrometry for identification of target napthenic acids using membrane sample inlets. We first investigated the interactions of the selected polymers with BEN and ISO molecules, which are known to penetrate the PDMS membrane efficiently.

The interaction energy between PDMS and CHA is significantly lower than that between PDMS and ISO, indicating that the pure PDMS might have the potential for practical applications as membrane material in the case of CHA. In the case of the 2NA molecule, the magnitude of the interaction energy with PDMS is just 0.5 kcal/-mol higher than the reference value.

At 300 K, all considered PDMS-based polymers may be suitable for CHA molecule, while in the case of the 2NA molecule, PDMS, PDMS-HDT and PDMS-TMT polymers may be suitable. Concerning the 2NA molecule, PDMS-B3T and PDMS-MHT might be suitable.

At 276 K, only PDMS, PDMS-HDT and PDMS-TMT might be potentially suitable for practical applications in the case of CHA. In the case of 2NA, at 276 K, the weakest interaction energy is again obtained in the case of the PDMS-TMT. At 343 K, the magnitude of interaction energies between all PDMS-based polymers and CHA molecule severely decreased below the reference value, with the lowest being again in the case of the PDMS-TMT. Interaction energy in the case of PDMS-TMT & CHA system severely approached interaction energy between PDMS and BEN at 300 K. At 343 K, interaction energies between PDMS, PDMS-HDT and PDMS-TMT were also weaker than the reference value. Other polymers had interaction energies that were just 0.2 kcal/mol and 0.5 kcal/mol stronger than the reference value.

DFTB analysis showed that the interaction energies between PDMS and CHA/2NA are not much stronger than those corresponding to the interaction between PDMS and ISO. Again, the PDMS-TMT provides the best results in the case of the CHA molecule, while the PDMS-B3T might be the best choice in the case of the 2NA molecule.

Analysis of noncovalent interactions by the DFT method shows that the weakest specific noncovalent interactions occur in the case of PDMS-TMT, considering conformations with the strongest interaction energies. The strong interaction energies in these cases are attributed to the highest number of formed noncovalent interactions. Besides PDMS, PDMS-TMT seems to have the highest potential for practical applications, because of which special attention was focused on the analysis of SAPT0 components of the interaction energy. The substitution of methyl group with hydrogen atom has been found to decrease the electrostatic component of interaction and raise the dispersion component of interaction, as elaborated in detail by considering the electronegativities, MEP surfaces, and atomic ESP charges.

CRediT authorship contribution statement

Stevan Armaković: Conceptualization, Methodology, Investigation, Writing – original draft, Writing – review & editing. **Đorđe Vujić:** Investigation, Writing – original draft, Writing – review & editing. **Boris Brkić:** Project administration, Investigation, Writing – original draft, Writing – review & editing.

Declaration of Competing Interest

The authors declare that they have no known competing financial interests or personal relationships that could have appeared to influence the work reported in this paper.

Acknowledgments

SA acknowledges the financial support of the Ministry of Education, Science and Technological Development of the Republic of Serbia (Grant No. 451-03-9/2021-14/200125).

Appendix A. Supplementary data

Supplementary data to this article can be found online at https://doi.org/10.1016/j.molliq.2022.118657.

References

[1] C. Wu, A. De Visscher, I.D. Gates, On naphthenic acids removal from crude oil and oil sands process-affected water, Fuel 253 (2019) 1229–1246, https://doi.org/10.1016/j.fuel.2019.05.091.
[2] R.D. Kane, M.S. Cayard, A comprehensive study on naphthenic acid corrosion, in: NACE - Int. Corros. Conf. Ser., 2002.
[3] M.P. Barrow, L.A. McDonnell, X. Feng, J. Walker, P.J. Derrick, Determination of the nature of naphthenic acids present in crude oils using nanospray Fourier transform ion cyclotron resonance mass spectrometry: The continued battle against corrosion, Anal. Chem. 75 (2003) 860–866, https://doi.org/10.1021/ac020388b.
[4] Y.Z. Wang, X.Y. Sun, Y.P. Liu, C.G. Liu, Removal of naphthenic acids from a diesel fuel by esterification, Energy Fuels 21 (2) (2007) 941–943, https://doi.org/10.1021/ef060501r10.1021/ef060501r.s001.
[5] K.E. Tollefsen, K. Petersen, S.J. Rowland, Toxicity of synthetic naphthenic acids and mixtures of these to fish liver cells, Environ. Sci. Technol. 46 (9) (2012) 5143–5150, https://doi.org/10.1021/es204124w.
[6] B. Fuhr, B. Banjac, T. Blackmore, P. Rahimi, Applicability of total acid number analysis to heavy oils and bitumens, in, Energy Fuels 21 (3) (2007) 1322–1324, https://doi.org/10.1021/ef0604285.
[7] G.C. Laredo, C.R. López, R.E. Álvarez, J.J. Castillo, J.L. Cano, Identification of naphthenic acids and other corrosivity-related characteristics in crude oil and vacuum gas oils from a Mexican refinery, Energy Fuels 18 (6) (2004) 1687–1694, https://doi.org/10.1021/ef034004b.
[8] E. Slavcheva, B. Shone, A. Turnbull, Review of naphthenic acid corrosion in oil refining, Br. Corros. J. 34 (2) (1999) 125–131, https://doi.org/10.1179/000705999101500761.
[9] M.P. Barrow, J.V. Headley, K.M. Peru, P.J. Derrick, Data visualization for the characterization of naphthenic acids within petroleum samples, Energy Fuels 23 (5) (2009) 2592–2599, https://doi.org/10.1021/ef800985z.
[10] J.V. Headley, D.W. McMartin, A review of the occurrence and fate of naphthenic acids in aquatic environments, J. Environ. Sci. Heal. - Part A Toxic/Hazardous Subst. Environ. Eng. 39 (2004) 1989–2010, https://doi.org/10.1081/ESE-120039370.
[11] X. Zhang, S. Wiseman, H. Yu, H. Liu, J.P. Giesy, M. Hecker, Assessing the toxicity of naphthenic acids using a microbial genome wide live cell reporter array system, Environ. Sci. Technol. 45 (5) (2011) 1984–1991, https://doi.org/10.1021/es1032579.

[12] R. Camilli, C.M. Reddy, D.R. Yoerger, B.A.S. Van Mooy, M.V. Jakuba, J.C. Kinsey, C.P. McIntyre, S.P. Sylva, J.V. Maloney, Tracking hydrocarbon plume transport and biodegradation at Deepwater Horizon, Science (80-) 330 (6001) (2010) 201–204.
[13] B. Brkić, N. France, S. Taylor, Oil-in-water monitoring using membrane inlet mass spectrometry, Anal. Chem. 83 (16) (2011) 6230–6236.
[14] B. Brkić, S. Giannoukos, S. Taylor, D.F. Lee, Mobile mass spectrometry for water quality monitoring of organic species present in nuclear waste ponds, Anal. Methods 10 (48) (2018) 5827–5833.
[15] M.O. Steinhauser, S. Hiermaier, A review of computational methods in materials science: examples from shock-wave and polymer physics, Int. J. Mol. Sci. 10 (2009) 5135–5216.
[16] G.R. Schleder, A.C.M. Padilha, C.M. Acosta, M. Costa, A. Fazzio, From DFT to machine learning: recent approaches to materials science–a review, J. Phys. Mater. 2 (2019) 32001, https://doi.org/10.1088/2515-7639/ab084b.
[17] T. Reichert, M. Vučićević, P. Hillman, M. Bleicher, S.J. Armaković, S. Armaković, Sumanene as a delivery system for 5-fluorouracil drug – DFT, SAPT and MD study, J. Mol. Liq. 342 (2021), https://doi.org/10.1016/j.molliq.2021.117526 117526.
[18] S.J. Armaković, Y.S. Mary, Y.S. Mary, S. Pelemiš, S. Armaković, Optoelectronic properties of the newly designed 1, 3, 5-triazine derivatives with isatin, chalcone and acridone moieties, Comput. Theor. Chem. 1197 (2021) 113160.
[19] F. Paularokiadoss, T. Christopher Jeyakumar, R. Thomas, A. Sekar, D. Bhakiaraj, Group 13 monohalides [AX (A = B, Al, Ga and In; X = Halogens)] as alternative ligands for carbonyl in organometallics: Electronic structure and bonding analysis, Comput. Theor. Chem. 1209 (2022) 113587, https://doi.org/10.1016/j.comptc.2021.113587.
[20] T. Pooventhiran, R. Thomas, U. Bhattacharyya, S. Sowrirajan, A. Irfan, D.J. Rao, Structural aspects, reactivity analysis, wavefunction based properties, cluster formation with helicene and subsequent detection from surface enhancement in Raman spectra of triclabendazole studies using first principle simulations, Vietnam J. Chem. 59 (2021) 887–901, https://doi.org/10.1002/vjch.202100067.
[21] A. Bielenica, S. Beegum, Y.S. Mary, Y.S. Mary, R. Thomas, S. Armaković, S.J. Armaković, S. Madeddu, M. Struga, C. Van Alsenoy, Experimental and computational analysis of 1-(4-chloro-3-nitrophenyl)-3-(3,4-dichlorophenyl) thiourea, J. Mol. Struct. 1205 (2020), https://doi.org/10.1016/j.molstruc.2019.127587.
[22] J. Stanojev, S. Armakovic, B. Bajac, J. Matovic, V.V. Srdic, PbSe sensitized with iodine and oxygen: a combined computational and experimental study, J. Alloys Compd. 896 (2022) 163119, https://doi.org/10.1016/j.jallcom.2021.163119.
[23] S. Jankov, S. Armaković, E. Tóth, V. Srdic, Z. Cvejic, S. Skuban, Electronic structure of yttrium-doped zinc ferrite–Insights from experiment and theory, J. Alloys Compd. 842 (2020) 155704, https://doi.org/10.1016/j.jallcom.2020.155704.
[24] S. Jankov, S. Armaković, E. Tóth, S. Skuban, V. Srdic, Z. Cvejic, Understanding how yttrium doping influences the properties of nickel ferrite – Combined experimental and computational study, Ceram. Int. 45 (2019), https://doi.org/10.1016/j.ceramint.2019.06.304.
[25] Y.S. Mary, V.S. Kumar, Y.S. Mary, R. K. S., R. Thomas, Detailed Quantum Mechanical Studies on Three Bioactive Benzimidazole Derivatives and Their Raman Enhancement on Adsorption over Graphene Sheets, Polycycl. Aromat. Compd. (2020) 1–10, https://doi.org/10.1080/10406638.2020.1852267.
[26] J.S. Al-Otaibi, Y.S. Mary, Y.S. Mary, R. Thomas, Evidence of cluster formation of pyrrole with mixed silver metal clusters, Agx-My (x = 4,5, y = 2/1 and M = Au/Ni/Cu) using DFT/SERS analysis, Comput. Theor. Chem. 1208 (2022), https://doi.org/10.1016/j.comptc.2021.113569 113569.
[27] J.S. Al-Otaibi, Y.S. Mary, Y.S. Mary, Adsorption of a thione bioactive derivative over different silver/gold clusters – DFT investigations, Comput. Theor. Chem. 1207 (2022), https://doi.org/10.1016/j.comptc.2021.113497 113497.
[28] J.S. Al-Otaibi, Y.S. Mary, Y.S. Mary, Z. Ullah, H.W. Kwon, Adsorption behavior and solvent effects of an adamantane-triazole derivative on metal clusters – DFT simulation studies, J. Mol. Liq. 345 (2022), https://doi.org/10.1016/j.molliq.2021.118242 118242.
[29] J.S. Al-Otaibi, Y.S. Mary, Y.S. Mary, R. Yadav, Structural and reactivity studies of pravadoline –An ionic liquid, with reference to its wavefunction-relative properties using DFT and MD simulation, J. Mol. Struct. 1245 (2021), https://doi.org/10.1016/j.molstruc.2021.131074 131074.
[30] M.K. Varghese, R. Thomas, N.V. Unnikrishnan, C. Sudarsanakumar, Molecular dynamics simulations of xDNA, Biopolymers 91 (5) (2009) 351–360, https://doi.org/10.1002/bip.21137.
[31] K.J. Bowers, D.E. Chow, H. Xu, R.O. Dror, M.P. Eastwood, B.A. Gregersen, J.L. Klepeis, I. Kolossvary, M.A. Moraes, F.D. Sacerdoti, Scalable algorithms for molecular dynamics simulations on commodity clusters, in: SC'06 Proc. 2006 ACM/IEEE Conf. Supercomput., IEEE, 2006: p. 43.
[32] A.D. Bochevarov, E. Harder, T.F. Hughes, J.R. Greenwood, D.A. Braden, D.M. Philipp, D. Rinaldo, M.D. Halls, J. Zhang, R.A. Friesner, Jaguar: A high-performance quantum chemistry software program with strengths in life and materials sciences, Int. J. Quantum Chem. 113 (2013) 2110–2142.
[33] L.D. Jacobson, A.D. Bochevarov, M.A. Watson, T.F. Hughes, D. Rinaldo, S. Ehrlich, T.B. Steinbrecher, S. Vaitheeswaran, D.M. Philipp, M.D. Halls, R.A. Friesner, Automated transition state search and its application to diverse types of organic reactions, J. Chem. Theory Comput. 13 (11) (2017) 5780–5797.
[34] Schrödinger Release 2021-4: Desmond Molecular Dynamics System, D. E. Shaw Research, New York, NY, 2021. Maestro-Desmond Interoperability Tools, Schrödinger, New York, NY, 2021., (n.d.).
[35] Schrödinger Release 2021-4: Jaguar, Schrödinger, LLC, New York, NY, 2021., (n.d.).
[36] E. Harder, W. Damm, J. Maple, C. Wu, M. Reboul, J.Y. Xiang, L. Wang, D. Lupyan, M.K. Dahlgren, J.L. Knight, OPLS3: a force field providing broad coverage of drug-like small molecules and proteins, J. Chem. Theory Comput. 12 (2016) 281–296.
[37] D. Shivakumar, J. Williams, Y. Wu, W. Damm, J. Shelley, W. Sherman, Prediction of absolute solvation free energies using molecular dynamics free energy perturbation and the OPLS force field, J. Chem. Theory Comput. 6 (5) (2010) 1509–1519.
[38] W.L. Jorgensen, D.S. Maxwell, J. Tirado-Rives, Development and testing of the OPLS all-atom force field on conformational energetics and properties of organic liquids, J. Am. Chem. Soc. 118 (45) (1996) 11225–11236.
[39] W.L. Jorgensen, J. Tirado-Rives, The OPLS [optimized potentials for liquid simulations] potential functions for proteins, energy minimizations for crystals of cyclic peptides and crambin, J. Am. Chem. Soc. 110 (6) (1988) 1657–1666.
[40] J.M. Martínez, L. Martínez, Packing optimization for automated generation of complex system's initial configurations for molecular dynamics and docking, J. Comput. Chem. 24 (7) (2003) 819–825.
[41] L. Martínez, R. Andrade, E.G. Birgin, J.M. Martínez, PACKMOL: a package for building initial configurations for molecular dynamics simulations, J. Comput. Chem. 30 (2009) 2157–2164.
[42] A.D. Becke, Density-functional thermochemistry. III. The role of exact exchange, J. Chem. Phys. 98 (7) (1993) 5648–5652, https://doi.org/10.1063/1.464913.
[43] P.C. Hariharan, J.A. Pople, The influence of polarization functions on molecular orbital hydrogenation energies, Theor. Chim. Acta. 28 (3) (1973) 213–222, https://doi.org/10.1007/BF00533485.
[44] W.J. Hehre, R. Ditchfield, J.A. Pople, Self—consistent molecular orbital methods. XII. Further extensions of Gaussian—type basis sets for use in molecular orbital studies of organic molecules, J. Chem. Phys. 56 (5) (1972) 2257–2261.
[45] R. Ditchfield, W.J. Hehre, J.A. Pople, Self-consistent molecular-orbital methods. IX. An extended Gaussian-type basis for molecular-orbital studies of organic molecules, J. Chem. Phys. 54 (2) (1971) 724–728.
[46] M. Elstner, D. Porezag, G. Jungnickel, J. Elsner, M. Haugk, T. Frauenheim, S. Suhai, G. Seifert, Self-consistent-charge density-functional tight-binding method for simulations of complex materials properties, Phys. Rev. B. 58 (1998) 7260.
[47] G. Seifert, D. Porezag, T.h. Frauenheim, Calculations of molecules, clusters, and solids with a simplified LCAO-DFT-LDA scheme, Int. J. Quantum Chem. 58 (2) (1996) 185–192.
[48] D. Porezag, T. Frauenheim, T. Köhler, G. Seifert, R. Kaschner, Construction of tight-binding-like potentials on the basis of density-functional theory: Application to carbon, Phys. Rev. B. 51 (1995) 12947.
[49] S. Grimme, C. Bannwarth, P. Shushkov, A robust and accurate tight-binding quantum chemical method for structures, vibrational frequencies, and noncovalent interactions of large molecular systems parametrized for all spd-block elements (Z= 1–86), J. Chem. Theory Comput. 13 (5) (2017) 1989–2009.
[50] E.G. Hohenstein, R.M. Parrish, C.D. Sherrill, J.M. Turney, H.F. Schaefer III, Large-scale symmetry-adapted perturbation theory computations via density fitting and Laplace transformation techniques: Investigating the fundamental forces of DNA-intercalator interactions, J. Chem. Phys. 135 (2011) 174107.
[51] E.G. Hohenstein, C.D. Sherrill, Density fitting and Cholesky decomposition approximations in symmetry-adapted perturbation theory: Implementation and application to probe the nature of π-π interactions in linear acenes, J. Chem. Phys. 132 (2010) 184111.
[52] B. Jeziorski, R. Moszynski, K. Szalewicz, Perturbation theory approach to intermolecular potential energy surfaces of van der Waals complexes, Chem. Rev. 94 (7) (1994) 1887–1930.
[53] E. Francisco, A.M. Pendás, Energy partition analyses: Symmetry-adapted perturbation theory and other techniques, in: Non-Covalent Interact. Quantum Chem. Phys., Elsevier, 2017, pp. 27–64.
[54] R. Rüger, M. Franchini, T. Trnka, A. Yakovlev, E. van Lenthe, P. Philipsen, T. van Vuren, B. Klumpers, T. Soini, AMS 2021.1 AMS 2021.1, SCM, Theoretical Chemistry, Vrije Universiteit, Amsterdam, The Netherlands, http://www.scm.com., (n.d.).
[55] R.M. Parrish, L.A. Burns, D.G.A. Smith, A.C. Simmonett, A.E. DePrince III, E.G. Hohenstein, U. Bozkaya, A.Y. Sokolov, R. Di Remigio, R.M. Richard, Psi4 1.1: An open-source electronic structure program emphasizing automation, advanced libraries, and interoperability, J. Chem. Theory Comput. 13 (2017) 3185–3197.
[56] J.M. Turney, A.C. Simmonett, R.M. Parrish, E.G. Hohenstein, F.A. Evangelista, J.T. Fermann, B.J. Mintz, L.A. Burns, J.J. Wilke, M.L. Abrams, N.J. Russ, M.L. Leininger, C.L. Janssen, E.T. Seidl, W.D. Allen, H.F. Schaefer, R.A. King, E.F. Valeev, C.D. Sherrill, T.D. Crawford, Psi4: an open-source ab initio electronic structure program, Wiley Interdiscip. Rev. Comput. Mol. Sci. 2 (4) (2012) 556–565.
[57] M.D. Hanwell, D.E. Curtis, D.C. Lonie, T. Vandermeersch, E. Zurek, G.R. Hutchison, Avogadro: an advanced semantic chemical editor, visualization, and analysis platform, J. Cheminform. 4 (2012) 17.
[58] Avogadro: an open-source molecular builder and visualization tool. Version 1.20. http://avogadro.cc/., (n.d.).
[59] E. Sokol, K.E. Edwards, K. Qian, R.G. Cooks, Rapid hydrocarbon analysis using a miniature rectilinear ion trap mass spectrometer, Analyst 133 (8) (2008) 1064, https://doi.org/10.1039/b805813j.

[60] C.A. Hughey, C.S. Minardi, S.A. Galasso-Roth, G.B. Paspalof, M.M. Mapolelo, R.P. Rodgers, A.G. Marshall, D.L. Ruderman, Naphthenic acids as indicators of crude oil biodegradation in soil, based on semi-quantitative electrospray ionization Fourier transform ion cyclotron resonance mass spectrometry, Rapid Commun. Mass Spectrom. An Int. J. Devoted to Rapid Dissem. Up-to-the-Minute Res. Mass Spectrom. 22 (2008) 3968–3976.
[61] P. Politzer, J.S. Murray, The fundamental nature and role of the electrostatic potential in atoms and molecules, Theor. Chem. Acc. 108 (3) (2002) 134–142.
[62] P. Politzer, J.S. Murray, F.A. Bulat, Average local ionization energy: a review, J. Mol. Model. 16 (11) (2010) 1731–1742.
[63] P. Sjoberg, P. Politzer, Use of the electrostatic potential at the molecular surface to interpret and predict nucleophilic processes, J. Phys. Chem. 94 (10) (1990) 3959–3961.
[64] J.S. Murray, P. Politzer, The electrostatic potential: an overview, Wiley Interdiscip. Rev. Comput. Mol. Sci. 1 (2) (2011) 153–163.
[65] P. Politzer, J.S. Murray, The average local ionization energy: concepts and applications, in: Theor. Comput. Chem.,, Elsevier, 2007, pp. 119–137.
[66] M.E. Bier, T. Kotiaho, R.G. Cooks, Direct insertion membrane probe for selective introduction of organic compounds into a mass spectrometer, Anal. Chim. Acta. 231 (1990) 175–190.
[67] R.A. Ketola, T. Kotiaho, M.E. Cisper, T.M. Allen, Environmental applications of membrane introduction mass spectrometry, J. Mass Spectrom. 37 (5) (2002) 457–476.
[68] 2-norbornaneacetic acid at ChemSpider, (n.d.). https://www.chemspider.com/Chemical-Structure.71470.html.
[69] Cyclohexanecarboxylic acid at ChemSpider, (n.d.). https://www.chemspider.com/Chemical-Structure.7135.html.
[70] A. Otero-de-la-Roza, E.R. Johnson, J. Contreras-García, Revealing non-covalent interactions in solids: NCI plots revisited, Phys. Chem. Chem. Phys. 14 (35) (2012) 12165, https://doi.org/10.1039/c2cp41395g.
[71] E.R. Johnson, S. Keinan, P. Mori-Sánchez, J. Contreras-García, A.J. Cohen, W. Yang, Revealing noncovalent interactions, J. Am. Chem. Soc. 132 (18) (2010) 6498–6506.